Environmental Science Nano

PAPER

View Article Online
View Journal | View Issue

Cite this: *Environ. Sci.: Nano*, 2015, 2, 653

Chronic dosing of a simulated pond ecosystem in indoor aquatic mesocosms: fate and transport of CeO_2 nanoparticles†

M. Tella,[ab] M. Auffan,*[ab] L. Brousset,[bc] E. Morel,[a] O. Proux,[d] C. Chanéac,[be] B. Angeletti,[ab] C. Pailles,[ab] E. Artells,[bc] C. Santaella,[bf] J. Rose,[ab] A. Thiéry[bc] and J.-Y. Bottero[ab]

Received 30th April 2015,
Accepted 5th September 2015

DOI: 10.1039/c5en00092k

rsc.li/es-nano

Indoor aquatic mesocosms were designed to mimic pond ecosystems contaminated by a continuous point-source discharge of cerium oxide nanoparticles (CeO_2-NPs). Bare and citrate-coated CeO_2-NPs exhibited different chemical and colloidal behaviors in the aquatic mesocosms. Bare CeO_2-NPs were chemically stable but quickly homo-aggregated and settled out of the water column. Citrate-coated NPs both homo- and hetero-aggregated but only after the several days required to degrade the citrate coating. While they were more stable as a colloidal suspension, coated CeO_2-NPs dissolved faster due to surface complexation with citrate, which resulted in the release of dissolved Ce into the water column. The different distributions over time between water/sediment or dissolved/particulate forms of Ce controlled the availability of Ce to benthic grazers (mollusk *Planorbarius corneus*) and planktonic filter feeders (copepod *Eudiaptomus vulgaris*).

Nano impact

Current strategies to assess the environmental safety of engineered nanomaterials are based on classical ecotoxicology approaches, which are not always adequate. Indeed, while the hazard is extensively investigated, little attention is paid to the exposure to nanomaterials despite its pivotal role in understanding their environmental risks. Indoor aquatic mesocosms were designed to mimic pond ecosystems contaminated by a continuous point-source discharge of CeO_2 nanoparticles. Geochemical modeling was combined with chemical analysis, time-resolved laser diffraction, and high-energy resolution fluorescence-detected X-ray absorption spectroscopy to adequately monitor the exposure of benthic and planktonic organisms in these mesocosms.

Introduction

The current global production of cerium oxide nanoparticles (CeO_2-NPs) is estimated to be ~10 000 tons,[1] with major CeO_2-NP producers located in Asia, Australia, and Europe. The primary industrial sectors in which CeO_2-NP technology is expected to be employed are electronics and optics, catalysts, energy and environment, coatings and paints.[2] Park *et al.* (2008) projected that 1255 tons of CeO_2 could be used in diesel fuel alone in the European Union in the year 2020.[3] Collin *et al.* (2014) estimated that adding CeO_2 to fuels could lead to a global CeO_2 consumption of 4400 tons per year, and 15–25% of CeO_2 in fuel additives is expected to be present as nanoparticles.[4] Keller *et al.* (2013) further estimated that 8200 tons per year of CeO_2 might be released to landfills, 1400 tons per year to soils, 100 tons per year to air, and 300 tons per year to water.[2] Once they are released into natural environments, the physico-chemical behavior of CeO_2-NPs will depend on environmental conditions (*e.g.* salinity, pH, dissolved organic matter, and natural colloids), nanoparticle properties (*e.g.* size, coating), and the product life cycle (*e.g.* formulation, use, and end of life), all of which will govern the exposure of organisms (*e.g.* micro- and macro-organisms, benthic and planktonic organisms) to CeO_2-NPs.

[a] *CNRS, Aix-Marseille Université, IRD, CEREGE UM34, UMR 7330, 13545 Aix-en-Provence, France. E-mail: auffan@cerege.fr*
[b] *International Consortium for the Environmental Implications of Nanotechnology (iCEINT), Aix-en-Provence, France*
[c] *Institut Méditerranéen de Biodiversité et d'Ecologie marine et continentale (IMBE), Aix Marseille Université, CNRS, IRD, Avignon Université UMR 7263, 13331 Marseille, France*
[d] *Observatoire des Sciences de l'Univers de Grenoble, UMS 832, CNRS, Université Joseph Fourier, 38041 Grenoble, France*
[e] *UPMC Univ Paris 06, CNRS, UMR 7574, Chimie de la Matière Condensée de Paris, Collège de France, 75231 Paris, France*
[f] *CNRS, Aix-Marseille Université, CEA, IBEB, Cadarache DSV/IBEB/SBVME, Lab Ecol Microb Rhizosphere & Environ Extrem (LEMiRE), UMR 7265, Saint-Paul-lez-Durance, France*

† Electronic supplementary information (ESI) available: Physico-chemical characterization of the nanoparticles and the kaolinites, characterization of the water column and sediments of the mesocosms (picoplankton, algae, physico-chemical parameters, and suspended matter), geochemical modeling, biovolume calculations, XANES of Ce in the water column, and HERFD-XAS set-up. See DOI: 10.1039/c5en00092k

To date, the thorough characterization of the colloidal and chemical stability of nanoparticles in the presence of biota and natural colloids at relevant concentrations over long periods of time remains challenging,[5] but a few studies have attempted to make headway in this area. One such study[6] focused on the exposure and environmental impact of a 1 mg L^{-1} pulse dose of CeO_2-NPs (4 nm) released to a simulated pond ecosystem. The authors successfully identified the interactions between the nanoparticles and naturally occurring (in)organic colloids and determined the distribution of CeO_2-NPs and dissolved Ce among the different compartments of the simulated ecosystem (aqueous phase, sediments, and biota). However, information is still needed regarding the role of particle size and coating in the aggregation and dissolution mechanisms and kinetics in this particular system. Moreover, Auffan *et al.* (2014) showed that the chosen contamination scenario (whether as runoff from rain or vent loading [*i.e.*, single pulse] or as a wastewater treatment plant or industrial discharge [*i.e.*, continuous or multiple dosing]) strongly controls the persistence of nanoparticles in the water column and uptake by organisms.[5] In the present study, we combine indoor aquatic mesocosms (*i.e.*, the simulated pond ecosystem) with geochemical modeling, time-resolved laser diffraction, and high-energy resolution fluorescence-detected X-ray absorption spectroscopy to adequately monitor the exposure of benthic and planktonic organisms to CeO_2-NPs during a continuous point-source discharge. Bare CeO_2-NPs and citrate-coated CeO_2-NPs available commercially as wood-stain adjuvants were used as potential contaminants to a simulated pond trophic system comprising primary producers (algae, bacteria) and primary consumers (mollusk *Planorbarius corneus* and copepod *Eudiaptomus vulgaris*). The chemical and colloidal stability of the CeO_2-NPs was thoroughly characterized, and the implications for uptake by the benthic and planktonic organisms were investigated.

Materials & methods

CeO_2 nanoparticle characteristics

Two commercially available types of CeO_2-NPs (bare and citrate-coated crystallites of ceria) were used in this study. The bare CeO_2-NPs (NanoGrain®, Umicore) had a primary particle size of 31 ± 18 nm (determined using TEM; see the ESI†), an average hydrodynamic diameter centered around 90 nm, a zeta potential of 42 ± 2 mV in the stock suspension (in ultrapure water at pH = 3.1), and an isoelectric point (IEP) of pH ~7.8 ± 2. Citrate-coated CeO_2-NPs (Nanobyk 3810®, BYK), sold as long-term UV stabilizers, were thoroughly described by Auffan *et al.* (2014).[7] Briefly, the citrate-coated CeO_2-NPs had a primary particle size of 3.9 ± 1.8 nm (determined using TEM; see the ESI†), an average hydrodynamic diameter centered around 8 nm, and a zeta potential of −40 ± 4 mV in ultrapure water from pH 3 to 10. The specific surface areas were estimated to be 56 ± 10 $m^2\ g^{-1}$ and 271 ± 177 $m^2\ g^{-1}$ for the 31 nm bare CeO_2-NPs and the 4 nm citrate-coated CeO_2-NPs, respectively. An additional batch of bare CeO_2-NPs with a primary particle size of 3–4 nm, an average hydrodynamic diameter centered around 8 nm (in ultrapure water at pH = 3.1), and an IEP between pH 7 and 7.5 was also used during batch experiments.[8]

Mesocosm set-up and monitoring

Nine indoor mesocosms (glass tanks of 750 × 200 × 600 mm) were set up to mimic a natural pond ecosystem. Natural sediments and organisms were collected from a non-contaminated pond in the preserved Natura 2000 reserve network in southern France (43.34361 N, 6.259663 E, altitude 107 m a.s.l.). Each mesocosm consisted of a layer of artificial sediment (79% SiO_2, 20% kaolinite, and 1% $CaCO_3$) covered with 300 g of water-saturated natural sediment containing primary producers (*e.g.*, algae, bacteria), and 46 L of Volvic® water with pH and conductivity values close to those of natural pond water (see Auffan *et al.* (2014)[5] for more details on the mesocosm set-up and monitoring). Three weeks of equilibration were necessary for the stabilization of the physicochemical parameters (pH, oxidation–reduction potential [ORP], dissolved O_2, and turbidity) in the mesocosms and the development of the primary producers. After the equilibration period, 11 mollusks (*P. corneus* (L. 1758), benthic grazers) and 200 copepods (*E. vulgaris* (Schmeil 1896), planktonic filter feeders) were introduced into each mesocosm. The organism density and male/female ratio were selected according to the natural biotope. Starting at day 0 (2 days after introduction of the organisms into the mesocosms), the water columns were dosed 3 times per week (on Monday, Wednesday, and Friday) for 4 weeks with 5.2 mg of CeO_2-NPs until day 28, resulting in a final concentration of 1.1 mg L^{-1} CeO_2-NPs and a total CeO_2 mass of 52.7 mg in the mesocosms. Three mesocosms were dosed with bare CeO_2-NPs, three were dosed with citrate-coated CeO_2-NPs, and three were kept as controls.

Details on the parameters monitored during the experiment for 7 weeks are provided in the ESI† and by Auffan *et al.* (2014).[5] Briefly, temperature (25.3 ± 0.6 °C), dissolved O_2 (7.4 ± 0.5 mg L^{-1}), pH (7.9 ± 0.1), and total organic carbon (2.0 ± 0.1 mg L^{-1}) were constant over time. ORP probes indicated that the water column was oxidative (241 ± 10 mV), while reductive conditions prevailed in sediments (−267 ± 15 mV). Conductivity increased during the experiment from 293 ± 8 μS cm^{-1} to 318 ± 15 μS cm^{-1} due to weekly refills with Volvic® water to compensate for evaporation. The concentrations of phosphates and carbonates were 3.8×10^{-6} mol L^{-1} and 0.2×10^{-3} mol L^{-1}, respectively, in the control mesocosms after 4 weeks. The primary producers were counted weekly in both the water column and sediments. The concentrations of picoplankton and algae were between 10^4–10^5 cells mL^{-1} and $<10^3$ cells mL^{-1} in the water column and between 10^6–10^7 cells mL^{-1} and 10^5–10^6 cells mL^{-1} at the surface of the sediments, respectively (see the ESI†). The concentration of particles with sizes ranging from 0.5 to 2.5 μm in the water

column was 10^6 particles mL^{-1}, as measured using an optical counter (HIAC).

Cerium quantification

The distribution of Ce in the mesocosms was quantified by measuring the Ce content in surficial sediments (depth of sampling estimated at about 0.9 ± 0.4 cm),[6] in the water column (at ~10 cm from the air/water interface and ~5 cm from the water/sediment interface), and in the organisms using ICP-MS (NexION 300X, Perkin Elmer) or ICP-AES (Jobin-Yvon Horiba). Surficial sediments and water were sampled at days 0, 1, 2, 7, 14, 21, and 28 (see Tella *et al.* (2014)[6] for experimental details about sample digestion and ICP analysis). Organisms were sampled weekly; at least 10 copepods from each mesocosm were collected, dried, and acid-digested at each time point. The weight of the copepods from each time point was determined by biovolume measurements[9] (see the ESI†). Adult *P. corneus* mollusks were dissected and their digestive glands were acid-digested (2 mL of HNO_3 and 1 mL of H_2O_2) before ICP-MS analysis. Each measurement was performed in triplicate, and the measurement quality was controlled using certified reference materials (estuarine sediment BCR-667 and mussel tissues BCR-668 from IRMM). All Ce concentrations presented are expressed in mg kg^{-1} (dry weight).

Cerium speciation

X-ray Absorption Near-Edge Structure (XANES) measurements were performed at the Ce L_3-edge on the CRG-FAME beamline at the ESRF (Grenoble, France) on water column and surficial sediment samples from day 28 of the experiment. For the water column, 6 L of water was ultracentrifuged (396 750*g* for 1 h), and the solid phase was freeze-dried. Spectral acquisition was performed at liquid helium temperature on freeze-dried samples to avoid sample evolution under the beam. Measurements were carried out in fluorescence mode using a Canberra Ge solid-state detector or a crystal analyzer spectrometer (see the ESI†).[10,11] Each spectrum was at least the sum of three scans. Data reduction was performed using an Ifeffit software package.[12] Initial bare and citrate-coated CeO_2-NPs and Ce^{III}–cysteine were used as Ce^{IV} and Ce^{III} reference samples. Ce^{III}–cysteine was laboratory-synthesized (equimolar solution of $Ce(SO_4)_2$ and L-cysteine at pH = 1).[13]

Solubility of CeO_2-NPs

Dialysis bags (10 kDa) were placed in the water column of the mesocosms to assess CeO_2-NP dissolution during the experiment. In addition, bare and coated CeO_2-NP suspensions were diluted to 1 mg L^{-1} in Volvic® water at pH 8 to study NP solubility in batch experiments. Bare CeO_2-NPs were diluted in 10^{-2} and 10^{-3} mol L^{-1} citrate solutions to assess the role of the citrate coating in CeO_2-NP dissolution. From 6 hours to 2 days, these suspensions were periodically ultrafiltered (Amicon tubes, 3 kDa) and dissolved Ce in the filtrate was measured by ICP-MS. The pH was monitored throughout the experiment.

Geochemical modeling of cerium speciation in the water column

Geochemical calculations were performed using the MEDUSA code[14] to predict phases that predominate in the pH and Eh range of the mesocosm water columns. Diagrams of the phase predominance of Ce were constructed with the aim of describing the equilibrium state of CeO_2-NPs in natural aqueous environments. The fixed activities of Ce and other components in the water column were used as input data.

CeO_2-NP homo- and hetero-aggregation

The initial size distribution and hetero-aggregation state of the kaolinite suspensions in Volvic® water in the presence of CeO_2-NPs (1 mg L^{-1}) were measured by laser diffractometry using a Mastersizer 3000 (Malvern, UK) in batch experiments. The concentration of kaolinite (20 mg L^{-1}; ~6×10^7 particles mL^{-1} between 0.5 and 2.5 μm) was chosen to be close to the number of particles in the water column of the mesocosms and in the detection range of the apparatus. Experiments were carried out in a system of well-controlled hydrological conditions in a 1 L beaker connected with plastic tubing to the measurement cell of the laser diffractometer. The experimental suspension was continuously pumped through the system at a constant rate of ~100 mL min^{-1}; the tubing was kept as short as possible to ensure reproducible conditions between different experiments and minimize the effect of shear in the tube on the aggregation kinetics.[15] Data are expressed in DV_{50} values which represent the volume-weighted median particle size. Homo-aggregation of the CeO_2-NP suspensions was also studied at 10 mg L^{-1} (concentration allowing good detection) in Volvic® water using NanoZS (Malvern, UK) and Mastersizer 3000 (Malvern, UK) instruments in batch experiments. Homo- and hetero-aggregation experiments were performed under daylight conditions at ambient temperature.

Results & discussion

Colloidal behavior of CeO_2-NPs in mesocosms

Distribution between the water column and the surficial sediments. Surface and deep waters were sampled 1.5 h, 3 h, 6 h, 24 h, and 48 h after the first injection of 5.2 mg of CeO_2-NPs (*i.e.* a Ce concentration of 100 μg L^{-1}) in each mesocosm. For bare CeO_2-NPs, a concentration gradient between the top (9.9 ± 0.9 μg L^{-1} at ~10 cm from the air/water interface) and the bottom of the water column (3 ± 1 μg L^{-1} at ~5 cm from the water/sediment interface) was observed after 1.5 h (Fig. 1a), after which the Ce concentration between the top and the bottom of the water column did not significantly evolve. 93 ± 3% of the Ce initially introduced at the top of the water column settled out of the water column after 48 h. For the coated CeO_2-NPs (Fig. 1b), a homogeneous Ce distribution (71 ± 12 μg L^{-1}) between the top and the bottom of

the water column was reached after 6 hours. Only 29 ± 12% of the Ce initially introduced had settled out after 48 h. These results highlight that waiting for 2 to 3 days between each dosing of NPs was enough to reach a steady state in terms of distribution in the water column.

After 4 weeks (Fig. 2), the total Ce concentration in the water column remained stable at 5 ± 2 μg L^{-1} and 49 ± 7 μg L^{-1} for bare and citrate-coated CeO_2-NPs, respectively. While the Ce concentration in the water column was ten times higher for the coated NPs than that for the bare NPs, similar Ce concentrations were measured in the surficial sediment for both types of CeO_2-NPs. The concentration in the sediment reached 99 ± 42 mg kg^{-1} after 4 weeks with a sedimentation rate of 1.0 ± 0.1 mg per day, which corresponds to ~99% (bare NPs) and ~75% (coated NPs) settling of Ce injected after 28 days. These percentages are in agreement with previous studies simulated using a single-pulse input of CeO_2-NPs[6,16] or Ag-NPs[17] in mesocosms. The factor of ~10 difference in the concentration of Ce in water after dosing with bare *versus* coated CeO_2-NPs and the longer time needed to obtain a homogeneous distribution of Ce in the water column for the coated CeO_2-NPs highlight different chemical and colloidal behaviors between these types of CeO_2-NPs (Fig. 1 and 2).

Homo-aggregation *versus* hetero-aggregation. Aggregation between particles can be modelled by the Smoluchowski equation (1917):[18]

$$dn/dt = -\alpha\beta(n, B)nB + K_B(n_0 - n)$$

with β as the product of the second-order collision rate constant, n as the concentration of unhetero-aggregated NPs, B as the concentration of background particles, and α as the affinity coefficient between nano- and background particles. The reverse reaction (breakup of larger aggregates into primary particles) can be assumed to be proportional (by the breakup rate constant K_B) to the number of NPs that have hetero-aggregated ($n_0 - n$). Recent work on homo- and hetero-aggregation has elucidated methods for distinguishing between α due to the two aggregation processes.[15,19–21] In the present study, changes in hydrodynamic diameters as a function of time were monitored to evaluate early-stage aggregation in both the homo- and hetero-aggregation scenarios.

Homo-aggregation was assessed in Volvic® water at pH 8 in batch experiments (Fig. 3). Bare CeO_2-NPs homo-aggregated in a few minutes and achieved an average hydrodynamic diameter of a few tens of microns within 4 h, whereas coated CeO_2-NPs remained more stable, with an average size below 1 μm after 180 hours (Fig. 3).[6] The faster homo-aggregation of the bare CeO_2-NPs can be explained by the IEP of these particles (at pH = 7.8 ± 2), which is close to the pH of the Volvic® water. The zeta potentials of the bare CeO_2-NPs measured under these pH and ionic strength conditions were about −2.6 ± 0.8 mV at 0.1 h and 5 ± 3 mV at 4.5 h. Based on Stokes' law, homo-aggregates of bare CeO_2-NPs with an average size of 30 μm would require less than 10 min to settle out in the mesocosm set-up, which is consistent with the fast kinetics of sedimentation of bare NPs measured by chemical analysis of the sediment (Fig. 1). However, the kinetics of homo-aggregation of the coated CeO_2-NPs were slower, likely due to the negatively charged coating that prevents homo-aggregation (Fig. 3). The zeta potentials of the coated CeO_2-NPs measured under these pH and ionic strength conditions evolved from −14 ± 4 mV at 0.1 h to 1 ± 0.1 mV at 180 h. Auffan *et al.* (2014)[7] demonstrated that citrate forms a chelate with Ce^{IV} through its central carboxyl and α-hydroxyl groups at the surface of the CeO_2-NPs. In the mesocosms, the citrate coating is degraded over time due to (i) strong dilution, which changes the chemical equilibrium and favors citrate desorption and (ii) the presence of daylight, which favors citrate degradation into acetate, oxalate, and other degradation by-products. Auffan *et al.* (2014)[7] measured an IEP of pH = 6 ± 1 for citrate-coated CeO_2-NPs after citrate degradation.[7] Consequently, the slow citrate-coated CeO_2-NP homo-aggregation observed in Volvic® water was likely due to degradation of the citrate coating.[6,7]

Natural colloids present in the mesocosm water (*e.g.* suspended clays, natural organic matter) can also cause the settling out of NPs through hetero-aggregation.[6,15,22,23] In the mesocosms, the number of colloids (mostly kaolinite

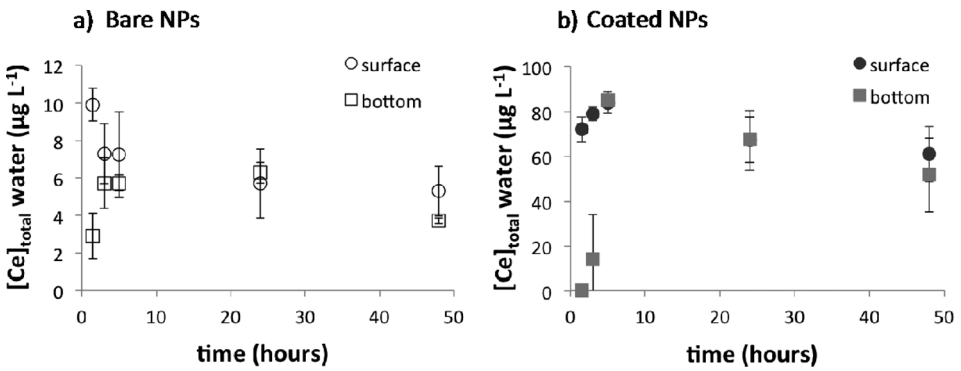

Fig. 1 Short-term distribution of cerium in the water column after the first input of 5.2 mg of bare cerium oxide nanoparticles (CeO_2-NPs) (a) and coated CeO_2-NPs (b). Water was sampled at ~10 cm from the air/water interface and at ~5 cm from the water/sediment interface. Data represent the average ± standard deviation of triplicates and are corrected from background concentration determined in control mesocosms.

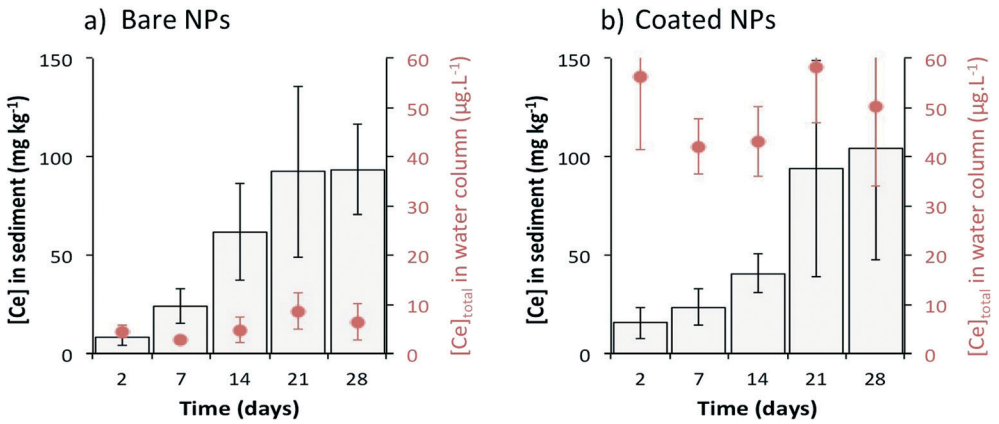

Fig. 2 Long-term distribution of Ce between the water column and the surficial sediments after 28 days of CeO_2-NP contamination for (a) bare CeO_2-NPs and (b) coated CeO_2-NPs. Water was sampled at ~10 cm from the air/water interface. Data represent the average of three replicates ± standard deviation and are corrected from background concentration determined in control mesocosms.

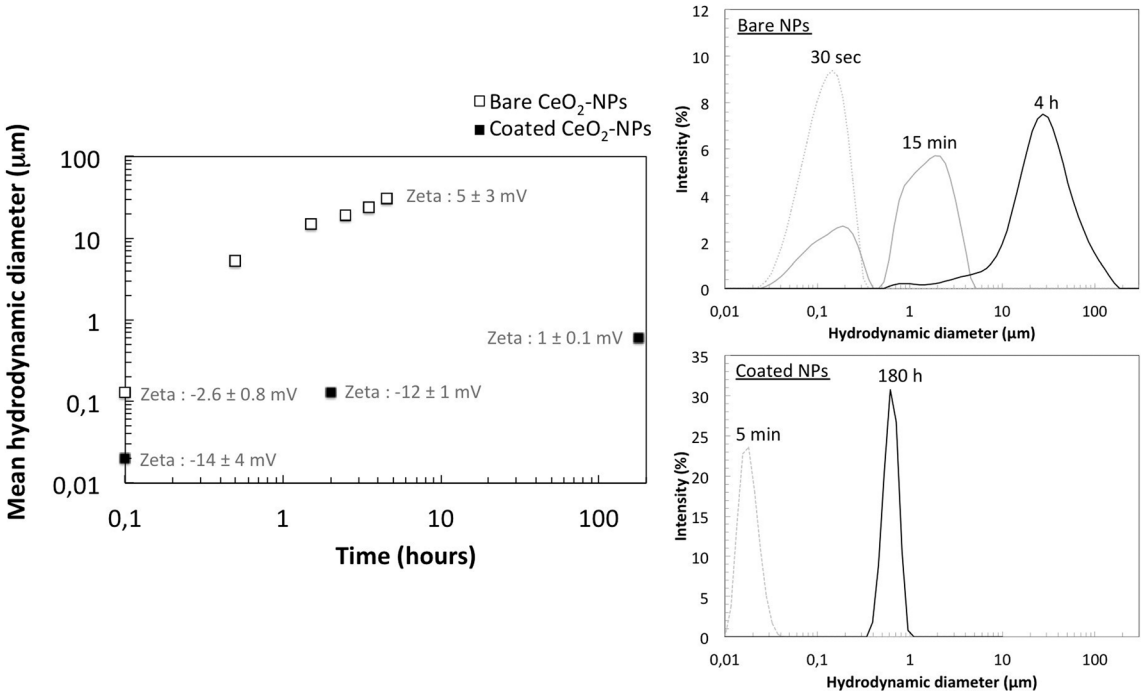

Fig. 3 Homo-aggregation of bare and citrate-coated cerium oxide nanoparticles (CeO_2-NPs) in Volvic® water at 10 mg L^{-1} in batch experiments. Zeta potential measurements were performed in Volvic® water (pH 7.9 ± 0.1).

particles) was close to 10^6 particles mL^{-1}, the number of bare CeO_2-NPs (31 ± 18 nm) between 10^9 particles mL^{-1} (for 0.1 mg L^{-1}) and 10^{10} particles mL^{-1} (for 1.1 mg L^{-1} at day 28), and the number of coated CeO_2-NPs (3.9 ± 1.8 nm) between 5 × 10^{11} particles mL^{-1} (for 0.1 mg L^{-1}) and 5 × 10^{12} particles mL^{-1} (for 1.1 mg L^{-1} at day 28). The interactions between kaolinite and bare or coated CeO_2-NPs were studied by time-resolved laser diffraction in Volvic® water at pH = 7.9 in batch experiments. Under these conditions, kaolinite particles formed stable homo-aggregates at about 16–17 µm (DV_{50}; see the ESI†). After injection of 1 mg L^{-1} CeO_2-NPs, a significant modification of the DV_{50} of the kaolinite occurred only with the 4 nm bare CeO_2-NPs (an increase of ~4.3 µm) and not with the 31 nm bare or 4 nm coated CeO_2-NPs (Fig. 4 and 5). Therefore, hetero-aggregation seems to be active only for small-sized bare NPs in conjunction with homo-aggregation. Fig. 4 and 5 also highlight that the degradation of the citrate present at the surface of the coated NPs needs to be taken into account for hetero-aggregation.[6,7] Indeed, coated CeO_2-NPs were aged for 3 days under daylight in Volvic® water (see ref. 6 and 7 for details) and were exposed to kaolinite particles. The aged coated NPs destabilized the kaolinite suspension 20 min after injection, with an increase of the DV_{50} by ~5 µm (Fig. 5). It is noteworthy that the aged coated

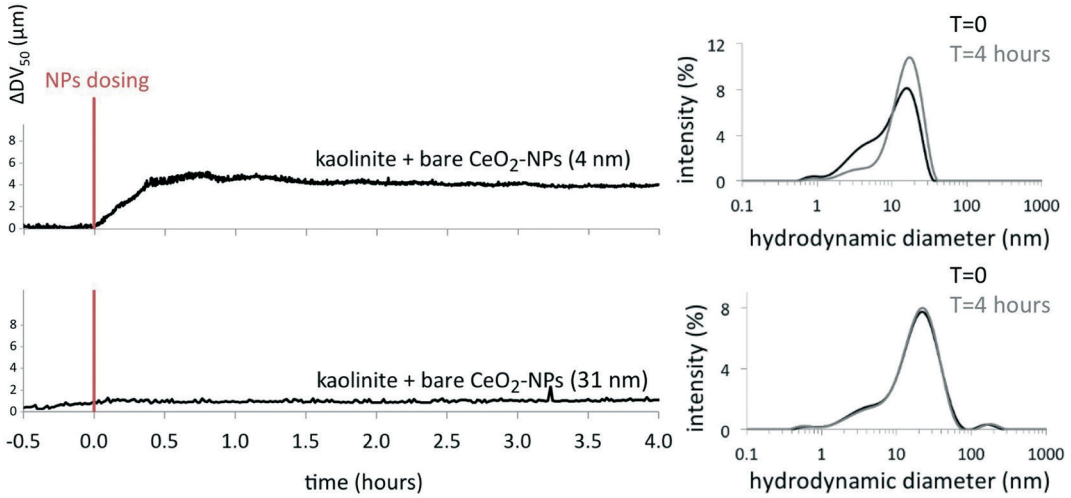

Fig. 4 Hetero-aggregation of bare cerium oxide nanoparticles (CeO_2-NPs) (~4 nm and ~31 nm) with kaolinite during batch experiments. The red line indicates the injection of 1 mg L^{-1} NPs into the kaolinite suspension (20 mg L^{-1}) in Volvic® water. Data are expressed in ΔDV_{50}, *i.e.* the volume-weighted median particle size at a given time subtracted from the volume-weighted median particle size of the kaolinite 30 min before NP dosing.

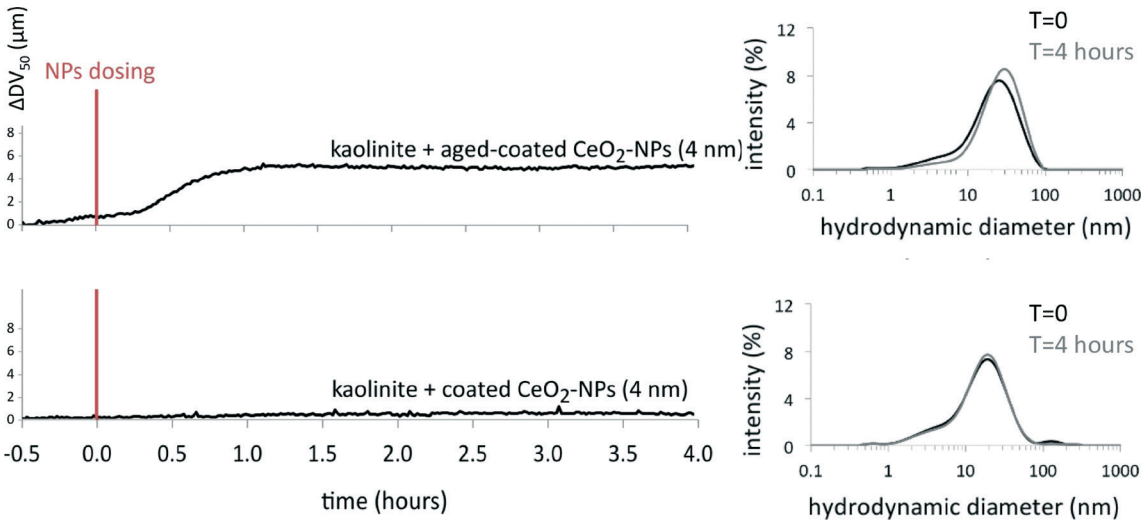

Fig. 5 Hetero-aggregation of initial and aged coated cerium oxide nanoparticles (CeO_2-NPs) with kaolinite during batch experiments. The red line indicates the injection of 1 mg L^{-1} NPs into the kaolinite suspension (20 mg L^{-1}) in Volvic® water. Data are expressed in ΔDV_{50}, *i.e.* the volume-weighted median particle size at a given time subtracted from the volume-weighted median particle size of the kaolinite 30 min before NP dosing.

NPs had a zeta potential close to that of the bare NPs,[7] but the bare NPs did not hetero-aggregate with the clays. The main difference between the two types of NPs is the primary particle size: 31 ± 18 nm for bare *versus* 4 ± 1 nm for aged coated CeO_2-NPs. The difference in primary particle size of the two types of particles consequently affects the respective particle numbers in the suspension (10^{10} particles mL^{-1} and 5×10^{12} particles mL^{-1} for the 31 nm bare and the 4 nm aged coated CeO_2-NPs, respectively). The ratio of NPs to kaolinites was determined to be ~500 times lower for the bare CeO_2-NPs than that for the aged coated CeO_2-NPs (based on the number of kaolinite particles between 0.5 and 2.5 μm of 6×10^7 particles mL^{-1}); this difference in availability of particle surfaces to interact with sites at the surface of the clays would be expected to result in a difference in the fate of the two types of CeO_2-NPs. Kaolinite is a 1 : 1-type aluminosilicate clay $[(Si_4)^{IV}(Al_4)^{VI}O_{10}(OH)_8]$ in which one tetrahedral sheet is combined with one octahedral sheet, forming a layer stack. This structure results in a crystal with a siloxane basal surface, an alumina basal surface with $>Al_2OH$ groups, and lateral surfaces with silanol (>SiOH) and aluminol (>AlOH) groups.[24] The charges of these lamellar particles are localized on the lateral surfaces[25] and can act as deposition sites that alter the fate of NPs in most aquatic systems. Based on the study by Sayed Hassan *et al.* (2005),[26] the average specific surface area of kaolinites is estimated at about 24 $m^2\ g^{-1}$, with 19 $m^2\ g^{-1}$ attributed to basal faces and 5 $m^2\ g^{-1}$ to lateral faces. Assuming that CeO_2-NPs interact specifically with the

more reactive lateral surfaces, we estimate that 20 mg L^{-1} of kaolinite corresponds to 0.10 m^2 L^{-1} of lateral surface available to interact with 0.03 m^2 L^{-1} of 31 nm bare NPs and 0.2 m^2 L^{-1} of 4 nm aged coated NPs. The partial coating of the lateral faces of kaolinite by CeO_2-NPs is then more favorable for the 4 nm aged coated NPs than for the 31 nm bare NPs. The chemical mechanism of hetero-aggregation at pH = 7.9 is related to the sorption of CeO_2-NPs through Ca^{2+} ion bridges between the negative lateral charges of kaolinite[25] and the neutral surfaces of the 4 nm bare CeO_2-NPs or the negative surfaces of the aged coated CeO_2-NPs.[7]

To conclude, two aggregation mechanisms co-occurred in the water column of the mesocosms. For 31 nm bare CeO_2-NPs, homo-aggregation appears to be the most favorable mechanism; these particles settled out very quickly due to the relative number of particles in suspension and particle surface charges. For coated CeO_2-NPs, both homo-aggregation and hetero-aggregation were favorable, but a few days under artificial daylight were required to degrade the citrate coating in the water column.

Chemical behavior of CeO_2-NPs in mesocosms

CeO_2-NP solubility in the water column. The concentration of dissolved Ce (<10 kDa) was measured in the water column of the mesocosms weekly over 28 days. The dissolved Ce concentration stabilized after 2 days at 1.1 ± 0.2 μg L^{-1} for bare (Fig. 6a) and 18 ± 2 μg L^{-1} for citrate-coated CeO_2-NPs (Fig. 6b), which correspond to 22 ± 4% and 36 ± 5% of the total Ce introduced, respectively. The strong chemical stability of bare CeO_2-NPs in the water column was also confirmed by XANES at the Ce L_3-edge at which Ce^{III} was not detected (see the ESI†). For both types of CeO_2-NPs, the concentrations of dissolved Ce measured in the mesocosms were not in agreement with the low solubility expected for Ce oxyhydroxide ($K_{sp,Ce(OH)_3}$ = 6.3 × 10^{-24} at 25 °C),[27] which suggests the presence of soluble inorganic or organic complexes of Ce in the mesocosms. The Ce speciation in the water column was geochemically modeled by considering the amount of cations and anions present in Volvic® water and the concentrations of phosphates and carbonates measured in the water column of the mesocosms. For bare CeO_2-NPs (Fig. 6c), the results of modeling are quantitatively in agreement with the Ce concentrations measured in the water column: Ce^{III}–CO_3^+ aqueous complexes represent 20% of the total Ce (*i.e.* 0.9 μg L^{-1}) in equilibrium with CeO_2(s) at pH = 7.9. However, these Ce^{III}–CO_3^+ complexes were not sufficient to account for the dissolved Ce measured in the mesocosms dosed with coated CeO_2-NPs (Fig. 6d). Another parameter that needed to be taken into account was the concentration of citrate present in

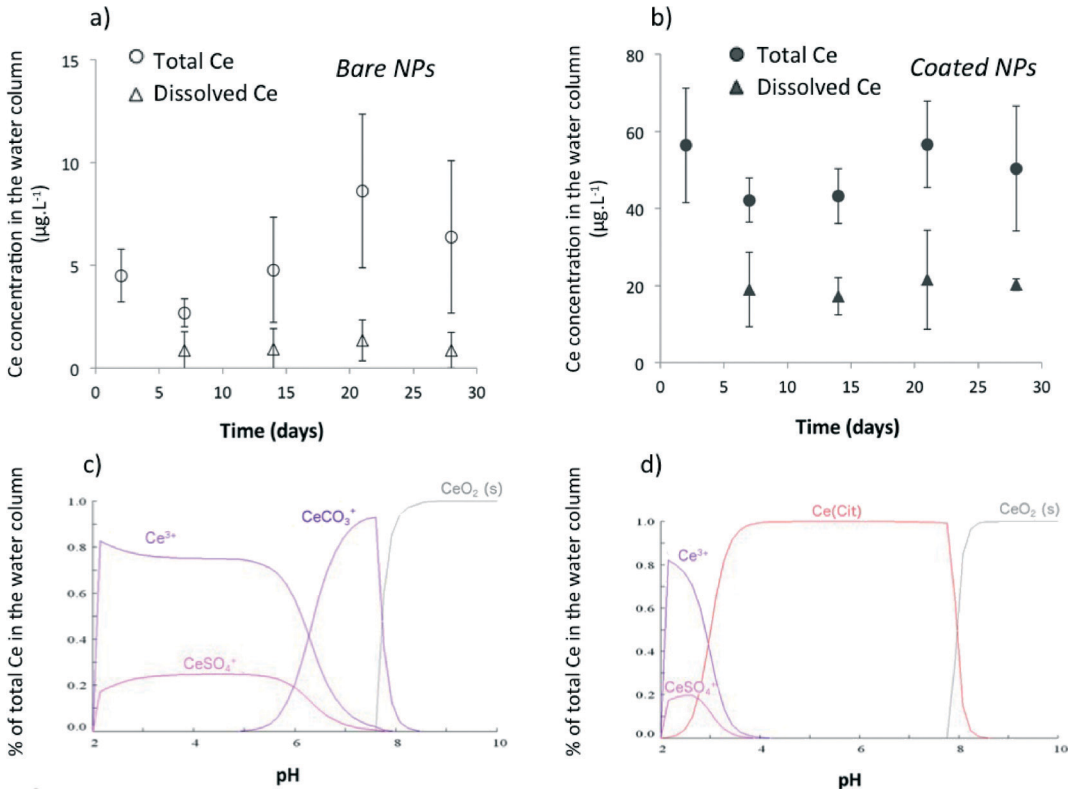

Fig. 6 Cerium (Ce) concentrations (total and dissolved) in the water column of the mesocosms (a, b) and the corresponding modeling for the bare (c) and citrate-coated cerium oxide nanoparticles (CeO_2-NPs) (d). For total Ce measurements, water was sampled at ~10 cm from the air/water interface. For dissolved Ce measurements, water was sampled in dialysis bags (10 kDa) introduced into the mesocosms. Data are the average of three replicates ± standard deviation and are corrected from background concentrations determined in control mesocosms. See the ESI† for the composition of the water column used for chemical modeling.

the stock suspension of the coated CeO_2-NPs.[6] An estimated concentration of 1.3×10^{-4} mol L^{-1} of citrate was introduced into the mesocosms during the injection of the coated CeO_2-NPs. The Ce speciation was then modeled by considering the Ce^{III}–Cit^0 complexes, and the results obtained were quantitatively in agreement with the Ce concentrations measured in the water column: Ce^{III}–Cit^0 aqueous complexes represent 70% of the total Ce (34 μg L^{-1}) in equilibrium with CeO_2(s) at pH = 7.9.

Role of citrate in CeO_2-NP chemical instability. To support the hypothesis that organic complexation of Ce surface atoms with citrate favors the dissolution of coated NPs in the mesocosms, batch experiments were carried out in Volvic® water. Bare CeO_2-NPs were incubated for 48 h with increasing concentrations of citric acid (0, 10^{-3}, and 10^{-2} mol L^{-1}) at pH = 8. In the absence of citric acid, dissolved Ce concentrations never exceeded the background concentration of Ce in the Volvic® water (0.5 ± 0.2 μg L^{-1}). In the presence of citrate, dissolved Ce concentrations rose to 76 ± 8 μg L^{-1} and 121 ± 14 μg L^{-1} for the 10^{-3} mol L^{-1} and 10^{-2} mol L^{-1} citrate solutions, respectively (Fig. 7). The increase of dissolved cerium in the presence of higher concentrations of citrate is in agreement with the formation of Ce^{III}–citrate complexes already observed.[28] All results demonstrated the presence of CeO_2(s) in equilibrium with $CeCO_3^+$ for bare CeO_2-NPs and $CeCit^0$ for coated CeO_2-NPs in the water column of the mesocosms.

Speciation of cerium in surficial sediments. Previous results have shown that surficial sediments accumulated ~99% (bare NPs) and ~75% (citrate-coated NPs) of Ce injected after 28 days. The speciation (local order and valence) of the Ce accumulated in these sediments was studied by X-ray Absorption Spectroscopy (XAS) at the Ce L_3-edge. However, standard transmission or total fluorescence XAS spectra do not have the required energy resolution to unambiguously identify Ce^{III} in the structure of CeO_2-NPs.[29] HERFD-XAS (High-Energy Resolution Fluorescence-Detected XAS) could address this deficiency[30] by offering more defined edge (Fig. 8a) and pre-edge (Fig. 8b) features for analysis. One of the most interesting features of HERFD-XAS is the ~2 eV difference between the pre-edges of Ce^{III} and Ce^{IV} reference compounds: 5719 eV for Ce^{III} and 5721 eV for Ce^{IV}. As shown in Fig. 8, the pre-edges of Ce in both samples were centered at 5721 eV, leading to the conclusion that no reduction of Ce^{IV} to Ce^{III} occurred in the surficial sediments after 28 days in the mesocosms.

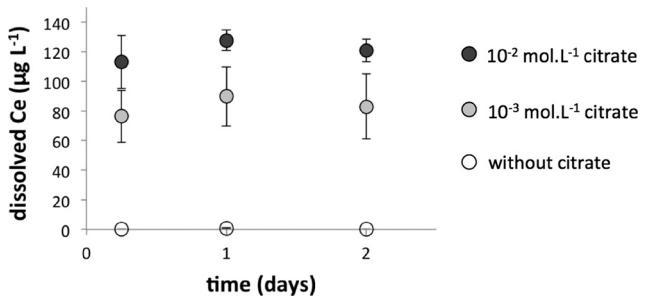

Fig. 7 Influence of citrate on the solubility of cerium oxide nanoparticles (CeO_2-NPs). Batch experiments were carried out in Volvic® water with 1 mg L^{-1} bare CeO_2-NPs (31 ± 18 nm). Dissolved cerium was measured after ultrafiltration of solutions at 3 kDa. Results indicate the average of three replicates ± standard deviation.

Implications of CeO_2-NP interactions with biota

All data presented for the chemical and colloidal behaviors of CeO_2-NPs in aquatic mesocosms after a continuous point-source discharge suggest drastically different fates for bare and citrate-coated CeO_2-NPs. Bare CeO_2-NPs quickly homo-aggregated (Fig. 3) and settled out (Fig. 2), but were chemically more stable (Fig. 6) than coated NPs, which dissolved faster due to surface complexation with citrate (Ce^{III}–Cit^0 complex, Fig. 6 and 7). Moreover, coated CeO_2-NPs required a few days of citrate-coating degradation before homo- and hetero-aggregation occurred (Fig. 3 and 4).

Table 1 presents the concentrations of Ce taken up or adsorbed onto the surface of *P. corneus* and *E. vulgaris* after exposure to bare and citrate-coated CeO_2-NPs. *Eudiaptomus* are planktonic filter feeders that pass water currents through sieve- or comb-like structures to feed.[31,32] The Ce concentrations in the copepods (whole organism) after 2 weeks were 288 ± 54 mg kg^{-1} (dry weight) and 3356 ± 625 mg kg^{-1} for bare and coated CeO_2-NPs, respectively. A similarly large amount was previously observed in *daphnia* after exposure to 0.1 mg L^{-1} TiO_2 NPs.[33] These planktonic filter feeders live and feed in the water column[32] and can ingest[34] and adsorb Ce on the cuticle.[35] The longer persistence of Ce in the water column after dosing with citrate-coated NPs is in agreement with the high amount of Ce measured in and/or on the surface of the copepods exposed to coated NPs. *Planorbarius* are benthic grazers that ate algae and biofilms at the sediment/water interface.[36] Consequently, the Ce concentration measured in their digestive glands depends on the Ce concentration in the surficial sediments and the settling kinetics of the homo- and hetero-aggregates. The Ce concentration measured in whole *P. corneus* was not statistically different between bare (2.1 ± 1.6 to 6.3 ± 6.0 mg kg^{-1}) and coated NPs (1.3 ± 0.9 to 5.1 ± 3.7 mg kg^{-1}) over time (Table 1), which is in agreement with the lack of statistically significant difference in Ce concentrations measured in surficial sediments.

In addition to ecological strategies, one important difference between *E. vulgaris* and *P. corneus* is the specific surface area (SSA) available to adsorb Ce. The small size and large SSA of *E. vulgaris* could explain why the concentration in the whole copepods is several orders of magnitude higher than that in the whole *P. corneus* mollusks.

Biodistribution was also investigated using XANES at the Ce L_3-edge to analyze Ce speciation in the digestive glands of *P. corneus* after 28 days. Significant reduction of Ce^{IV} to Ce^{III} was observed for both bare and coated CeO_2-NPs in the digestive glands (Fig. 8c). A peak appeared on the

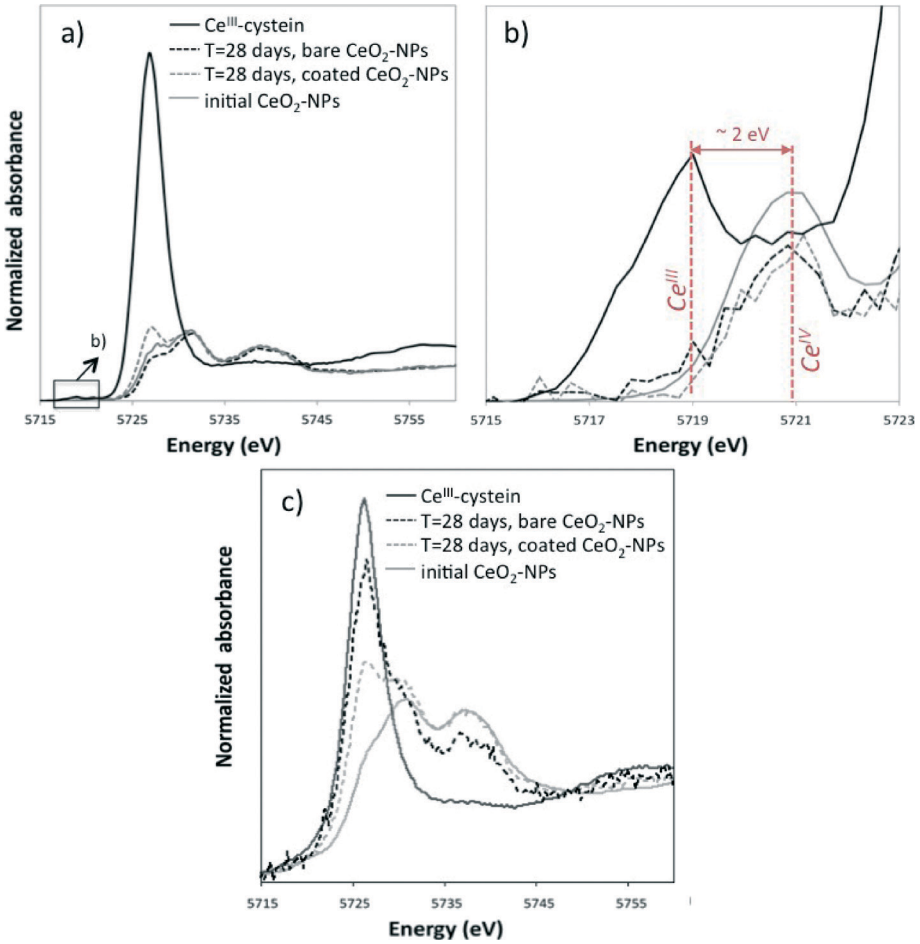

Fig. 8 Cerium (Ce) L_3-edge X-ray absorption near-edge structure (XANES) spectra of Ce accumulated on the surficial sediments (using high-energy resolution fluorescence-detected XAS [HERFD-XAS]) (a, b) and in the digestive gland of *Planorbarius corneus* at day 28 (total fluorescence XAS) (c). Details of the pre-edge area are shown in (b). Experimental spectra are compared to Ce^{III}–cysteine and initial nanoparticle reference spectra.

Table 1 Concentration of cerium (Ce) (mg kg^{-1} dry weight) measured in whole planktonic *Eudiaptomus* copepods as well as in whole benthic *Planorbarius* mollusks and their digestive gland exposed to cerium oxide nanoparticles (CeO_2-NPs) over 28 days in mesocosms. For copepods, masses were estimated from biovolumes considering 20% of dry matter in organisms. DG: Digestive gland. N/A: Not analyzed

	Bare CeO_2-NPs			Coated CeO_2-NPs		
	Planktonic	Benthic		Planktonic	Benthic	
	Whole	Whole	DG	Whole	Whole	DG
7 d	288 ± 54	2.1 ± 1.6	31 ± 25	97 ± 18	5.1 ± 3.7	82 ± 62
14 d	111 ± 21	6.3 ± 6.0	170 ± 170	3356 ± 625	1.6 ± 1.1	16 ± 18
21 d	N/A	4.4 ± 4.1	140 ± 130	N/A	1.3 ± 0.9	9 ± 8
28 d	N/A	2.8 ± N/A	85 ± N/A	N/A	3.4 ± 2.4	60 ± 42

XANES spectra of CeO_2-NPs at the energy of the edge observed for the Ce^{III}–cysteine reference compound (Fig. 8c). The intensity of the peak is higher for bare CeO_2-NPs than that for coated CeO_2-NPs, highlighting the more important bioreduction of Ce following bare CeO_2-NP ingestion. However, the XAS spectra acquired in total fluorescence do not have the required energy resolution to quantitatively determine the percentage of Ce^{III} in the structure of the NPs.[29]

Conclusions

The thorough characterization of the fate and transport of CeO_2-NPs presented in the current study highlights not only the physico-chemical mechanisms and kinetics of transformation and distribution which vary in complex ecosystems due to the differences in the size and surface properties of the NPs but also the kinetics and mechanisms of homo-aggregation, hetero-aggregation, Ce^{III}–organic complexation,

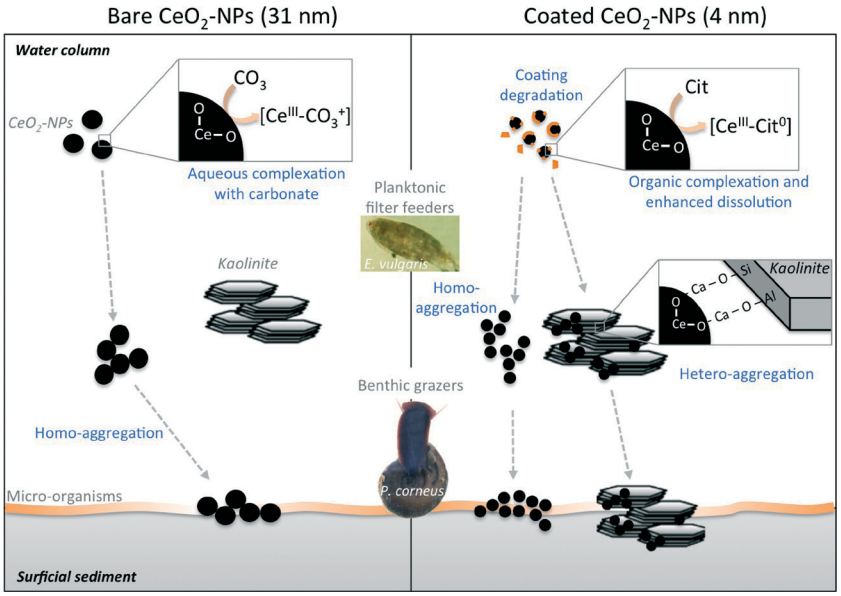

Fig. 9 Scheme highlighting the physico-chemical mechanisms which affect the fate of cerium oxide nanoparticles in the mesocosms (*e.g.* homo-aggregation, hetero-aggregation, dissolution, complexation with organic compounds, and coating degradation) in relation to the ecological strategies of the organisms.

dissolution, and coating degradation. The degree to which these factors influence the exposure and uptake of CeO_2-NPs by organisms will also be determined by ecological strategies (*e.g.* benthic *versus* planktonic, filter feeders *versus* grazers) (Fig. 9), which suggests the need to further investigate significant differences in biological impacts on micro- and macro-organisms with different ecological traits and strategies. In addition, this study focused only on the first two links of a lentic water trophic chain: the producers (diatoms, green algae, and biofilm) and the first consumers (filter feeders in the water column and benthic grazers on sediments). For a better understanding of the impacts on the food chain, the predators (*i.e.* secondary consumers [*e.g.* dragonflies, water beetles]) should be investigated. Furthermore, the selected organisms were arbitrarily chosen at the adult developmental stage. The fate of CeO_2-NPs in systems with newly hatched forms (*e.g.* nauplius and copepodid phases for copepods, shell-less gastropods) should be investigated.

Acknowledgements

The authors would like to thank Raisa Tikhtman and Anne Pariat for their help during the experiments and Helene Miche for the phosphate concentration determination. We also thank Jerome Labille for the discussions we had about hetero-aggregation and Amalia Turner who revised the manuscript. The authors thank the CNRS for funding the GDRi-iCEINT, and the French ANR for funding the ANR-10-NANO-0006/MESONNET project. This work is a contribution to the Labex Serenade (ANR-11-LABX-0064) funded by the «Investissements d'Avenir» French Government program of the French National Research Agency (ANR) through the A*MIDEX project (ANR-11-IDEX-0001-02). The Ge(331) bent crystals used for the HERDF measurements were partially funded by a grant from Labex OSUG@2020 (ANR-10-LABX-0056). The authors acknowledge financial support provided by the FP7 project NANoREG (a common European approach to the regulatory testing of manufactured nanomaterials; European Commission, grant agreement number 310584) and the OSU-Institut pythéas.

Notes and references

1 European Commission, 2012.
2 A. Keller, S. McFerran, A. Lazareva and S. Suh, *J. Nanopart. Res.*, 2013, **15**, 1–17.
3 B. Park, K. Donaldson, R. Duffin, L. Tran, F. Kelly, I. Mudway, J.-P. Morin, R. Guest, P. Jenkinson, Z. Samaras, M. Giannouli, H. Kouridis and P. Martin, *Inhalation Toxicol.*, 2008, **20**, 547–566.
4 B. Collin, M. Auffan, A. C. Johnson, I. Kaur, A. A. Keller, A. Lazareva, J. R. Lead, X. Ma, R. C. Merrifield, C. Svendsen, J. C. White and J. M. Unrine, *Environ. Sci.: Nano*, 2014, **1**, 533–548.
5 M. Auffan, M. Tella, C. Santaella, L. Brousset, C. Pailles, M. Barakat, B. Espinasse, E. Artells, J. Issartel, A. Masion, J. Rose, M. Wiesner, W. Achouak, A. Thiéry and J.-Y. Bottero, *Sci. Rep.*, 2014, **4**, 5608.
6 M. Tella, M. Auffan, L. Brousset, J. Issartel, I. Kieffer, C. Pailles, E. Morel, C. Santaella, B. Angeletti, E. Artells, J. Rose, A. Thiéry and J.-Y. Bottero, *Environ. Sci. Technol.*, 2014, **48**, 9004–9013.
7 M. Auffan, A. Masion, J. Labille, M. A. Diot, W. Liu, L. Olivi, O. Proux, F. Ziarelli, P. Chaurand, C. Geantet, J.-Y. Bottero and J. Rose, *Environ. Pollut.*, 2014, **188**, 1–7.
8 M. A. Diot, *Aix-Marseille*, 2012.
9 J. Sun and D. Liu, *J. Plankton Res.*, 2003, **25**, 1331–1346.

10 J.-L. Hazemann, O. Proux, V. Nassif, H. Palancher, E. Lahera, C. Da Silva, A. Braillard, D. Testemale, M.-A. Diot, I. Alliot, W. Del Net, A. Manceau, F. Gelebart, M. Morand, Q. Dermigny and A. Shukla, *J. Synchrotron Radiat.*, 2009, **16**, 283–292.
11 I. Llorens, E. Lahera, W. Delnet, O. Proux, A. Braillard, J.-L. Hazemann, A. Prat, D. Testemale, Q. Dermigny, F. Gelebart, M. Morand, A. Shukla, N. Bardou, O. Ulrich, S. Arnaud, J.-F. Berar, N. Boudet, B. Caillot, P. Chaurand, J. Rose, E. Doelsch, P. Martin and P. L. Solari, *Rev. Sci. Instrum.*, 2012, **83**, 063104.
12 B. Ravel and M. Newville, *J. Synchrotron Radiat.*, 2005, **12**, 537–541.
13 G.-C. Han, Y. Peng, Y.-Q. Hao, Y.-N. Liu and F. Zhou, *Anal. Chim. Acta*, 2010, 659.
14 in *219th ACS National Meeting, Abstract of Papers*, ed. I. Puigdomenech, A. C. Society, San Francisco, 2000, vol. 1.
15 A. Praetorius, J. Labille, M. Scheringer, A. Thill, K. Hungerbuhler and J. Y. Bottero, *Environ. Sci. Technol.*, 2014, **48**, 10690–10698.
16 P. Zhang, X. He, Y. Ma, K. Lu, Y. Zhao and Z. Zhang, *Chemosphere*, 2012, **89**, 530–535.
17 G. V. Lowry, B. P. Espinasse, A. R. Badireddy, C. J. Richardson, B. C. Reinsch, L. D. Bryant, A. J. Bone, A. Deonarine, S. Chae, M. Therezien, B. P. Colman, H. Hsu-Kim, E. S. Bernhardt, C. W. Matson and M. R. Wiesner, *Environ. Sci. Technol.*, 2012, **46**, 7027–7036.
18 V. Z. Smoluchowski, Mathematical Theory of the Kinetics of the Coagulation of Colloidal Suspensions, *Phys. Chem. Chem. Phys.*, 1917, **92**, 129.
19 L. Barton, M. Therezien, M. Auffan, J.-Y. Bottero and M. Wiesner, *Environ. Eng. Sci.*, 2014, **31**, 421–427.
20 M. Therezien, A. Thill and M. R. Wiesner, *Sci. Total Environ.*, 2014, **485–486**, 309–318.
21 J. Labille, C. Harns, J.-Y. Bottero and J. Brant, Heteroaggregation of Titanium Dioxide Nanoparticles with Natural Clay Colloids, *Environ. Sci. Technol.*, 2015, **49**(11), 6608–6616.
22 D. Zhou, A. I. Abdel-Fattah and A. A. Keller, *Environ. Sci. Technol.*, 2012, **46**, 7520–7526.
23 J. Zhao, F. Liu, Z. Wang, X. Cao and B. Xing, *Environ. Sci. Technol.*, 2015, **49**, 2849–2857.
24 M. F. Brigatti, E. Galan and B. K. G. Theng, in *Handbook of Clay Science. Developments in Clay Science*, ed. F. Bergaya, G. K. B. Theng and G. Lagaly, Elsevier, Amsterdam, 2006, vol. 1, pp. 19–86.
25 E. Tombacz and M. Szekeres, *Appl. Clay Sci.*, 2006, **34**, 105–124.
26 M. Sayed Hassan, F. Villieras, A. Razafitianamaharavo and L. Michot, *Langmuir*, 2005, **21**, 12283–12289.
27 in *Basic Principles and Industrial Applications*, ed. O. Söhnel and J. Garside, Butterworth-Heinemann, Boston, 1992, p. 149.
28 *NIST*, ed. R. M. Smith and A. E. Martell, 2004, vol. 8.
29 A. M. Shahin, F. Grandjean, G. J. Long and T. P. Schuman, *Chem. Mater.*, 2005, **17**, 315–321.
30 J.-D. Cafun, K. O. Kvashnina, E. Casals, V. F. Puntes and P. Glatzel, *ACS Nano*, 2013, **7**, 10726–10732.
31 G.-A. Paffenhöfer and K. D. Lewis, *J. Plankton Res.*, 1990, **12**, 933–946.
32 U. Sommer and F. Sommer, *Oecologia*, 2006, **147**, 183–194.
33 X. Zhu, Y. Chang and Y. Chen, *Chemosphere*, 2010, **78**, 209–215.
34 M. Auffan, D. Bertin, P. Chaurand, C. Pailles, C. Dominici, J. Rose, J.-Y. Bottero and A. Thiéry, *Water Res.*, 2013, **47**, 3921–3930.
35 E. Artells, J. Issartel, M. Auffan, D. Borschneck, A. Thill, M. Tella, L. Brousset, J. Rose, J.-Y. Bottero and A. Thiéry, *PLoS One*, 2013, **8**, e71260.
36 J. B. Graham, *Integr. Comp. Biol.*, 1990, **30**, 137–146.